Mechanistic Studies on *N*-Acetylmuramic Acid 6-Phosphate Hydrolase (MurQ): An Etherase Involved in Peptidoglycan Recycling[†]

Timin Hadi,[‡] Ulrike Dahl,[§] Christoph Mayer,[§] and Martin E. Tanner*,[‡]

Department of Chemistry, University of British Columbia, Vancouver, British Columbia, Canada V6T 1Z1, and Fachbereich Biologie, Molekulare Mikrobiologie, Universität Konstanz, Universitätsstrasse 10, 78457 Konstanz, Germany

Received August 1, 2008; Revised Manuscript Received August 29, 2008

ABSTRACT: Peptidoglycan recycling is a process in which bacteria import cell wall degradation products and incorporate them back into either peptidoglycan biosynthesis or basic metabolic pathways. The enzyme MurQ is an *N*-acetylmuramic acid 6-phosphate (MurNAc 6-phosphate) hydrolase (or etherase) that hydrolyzes the lactyl side chain from MurNAc 6-phosphate and generates GlcNAc 6-phosphate. This study supports a mechanism involving the *syn* elimination of lactate to give an α,*β*-unsaturated aldehyde with (*E*)-stereochemistry, followed by the *syn* addition of water to give product. The observation of both a kinetic isotope effect slowing the reaction of [2-^{2}H]MurNAc 6-phosphate and the incorporation of solvent-derived deuterium into C2 of the product indicates that the C2−H bond is cleaved during catalysis. The observation that the solvent-derived ^{18}O isotope is incorporated into the C3 position of the product, but not the C1 position, provides evidence of the cleavage of the C3−O bond and argues against imine formation. The finding that 3-chloro-3-deoxy-GlcNAc 6-phosphate serves as an alternate substrate is also consistent with an elimination−addition mechanism. Upon extended incubations of MurQ with GlcNAc 6-phosphate, the α,*β*-unsaturated aldehydic intermediate accumulates in solution, and ^{1}H NMR analysis indicates it exists as the ring-closed form of the (*E*)-alkene. A structural model is developed for the *Escherichia coli* MurQ and is compared to that of the structural homologue glucosamine-6-phosphate synthase. Putative active site acid/base residues are probed by mutagenesis, and Glu83 and Glu114 are found to be crucial for catalysis. The Glu83Ala mutant is essentially inactive as an etherase yet is capable of exchanging the C2 proton of substrate with solvent-derived deuterium. This suggests that Glu83 may function as the acidic residue that protonates the departing lactate.

Peptidoglycan is a key structural component of the bacterial cell wall and is required to protect the bacteria from lysis due to osmotic pressure (*1, 2*). During bacterial growth, peptidoglycan biosynthesis and peptidoglycan breakdown make up a dynamic process and must be carefully balanced to meet the needs of the organism (*3*). In certain bacteria, such as *Escherichia coli*, a complex system of enzymes and proteins has developed that is responsible for importing and recycling cell wall components formed during peptidoglycan breakdown (*4*). These components may be reused in further peptidoglycan biosynthesis or shuttled into basic metabolic pathways. The peptidoglycan structure is defined by polysaccharide chains comprised of alternating residues of *N*-acetylglucosamine (GlcNAc)[1] and its 3-*O*-lactyl ether derivative, *N*-acetylmuramic acid (MurNAc) (Figure 1). These polysaccharide chains are cross-linked via peptide bridges attached to the MurNAc residues. During cell wall degradation and recycling, lytic transglycosylases and endopeptidases

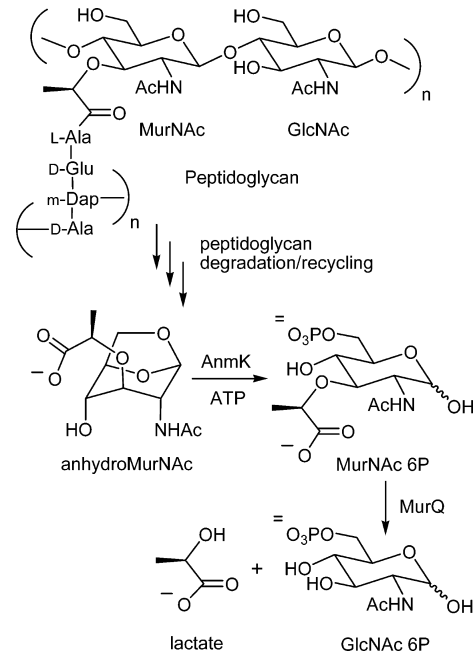

FIGURE 1: Formation of anhydroMurNAc during peptidoglycan recycling and its conversion into GlcNAc 6-phosphate and lactate by the enzymes AnmK and MurQ.

[†] This research was supported by the Natural Sciences and Engineering Research Council of Canada (NSERC) (M.E.T.) and the Deutsche Forschungsgemeinschaft (Heisenberg fellowship and Grant MA2436 to C.M.).

* To whom correspondence should be addressed. Phone: (604) 822-9453. Fax: (604) 822-2847. E-mail: mtanner@chem.ubc.ca.

[‡] University of British Columbia.

[§] Universität Konstanz.

[1] Abbreviations: GlcNAc, *N*-acetylglucosamine; GlmS, glucosamine 6-phosphate synthase; INT, *p*-iodonitrotetrazolium violet; KIE, kinetic isotope effect; MurNAc, *N*-acetylmuramic acid; 6P, 6-phosphate; SIS, sugar isomerase; Trien, triethanolamine.

10.1021/bi8014532 CCC: $40.75
Published on Web 10/07/2008

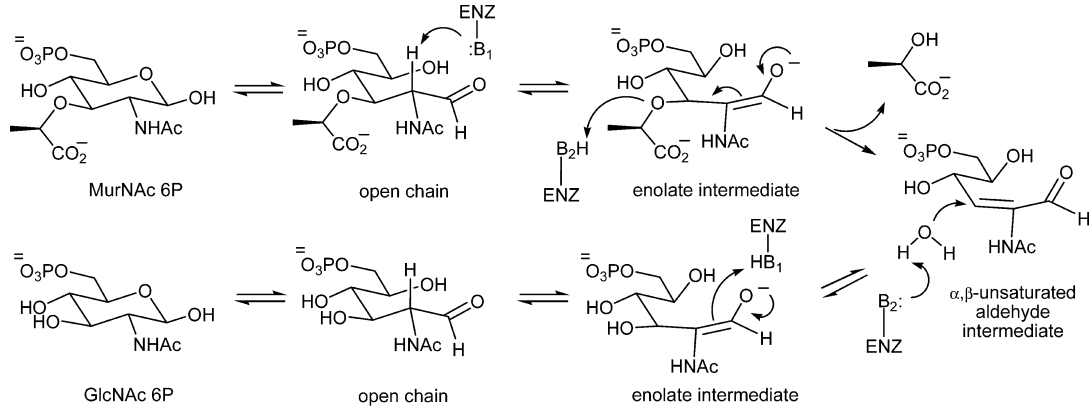

FIGURE 2: Mechanism of the reaction catalyzed by the MurNAc 6-phosphate hydrolase (MurQ).

break the peptidoglycan into disaccharide−peptide fragments that are transported across the inner membrane into the cytoplasm (*4, 5*). Further cytoplasmic recycling enzymes cleave the glycosidic and peptidic bonds to release the individual sugars and amino acids. The fate of the MurNAc residue is unusual in that it is initially generated as a 1,6-anhydro sugar (this linkage is formed during cleavage of the MurNAc−GlcNAc bond). Recent studies have uncovered two enzymes responsible for converting anhydroMurNAc into the common metabolic intermediate, GlcNAc 6-phosphate, which can ultimately be shuttled into glycolysis (Figure 1) (*6*). The first is a bifunctional enzyme, AnmK, which serves to hydrolyze the 1,6-anhydro−glycosidic linkage and to subsequently phosphorylate the C6 position, giving MurNAc 6-phosphate. The second is MurQ, an *N*-acetylmuramic acid 6-phosphate hydrolase (this enzyme has also been called a lyase or etherase) that converts MurNAc 6-phosphate into GlcNAc 6-phosphate and lactic acid (*7*−*9*). As ether bonds are normally not subject to rapid hydrolysis, the ability of MurQ to act as an "etherase" presents an interesting subject for mechanistic studies (*10*).

The proposed mechanism for the MurQ reaction begins with a facile ring opening of MurNAc 6-phosphate, which is likely enzyme-catalyzed and generates the open chain aldehyde (Figure 2) (*7, 9*). This serves to acidify the proton at C2 and permits deprotonation by an active site base (B_1 in Figure 2) and the generation of an enolate intermediate. The loss of lactate then occurs with the aid of an active site acidic residue (B_2 in Figure 2) that protonates the departing oxygen. This overall elimination of lactate generates an α,β-unsaturated aldehyde intermediate of unknown stereochemistry. Under normal conditions, the release of lactate is expected to be effectively irreversible as lactate is present at a much lower concentration than water. The second half of the reaction is largely a mirror of the first involving a conjugate addition of water onto the α,β-unsaturated aldehyde. It is expected that the same two acid/base residues are positioned appropriately to deprotonate the water molecule (B_2) and to deliver a proton to C2 of the enolate intermediate (B_1). Ring closure to give the product GlcNAc 6-phosphate could be enzyme-catalyzed or occur spontaneously in solution.

Past work on the mechanism of MurQ is entirely consistent with this mechanism. When the reaction was conducted in $H_2{}^{18}O$, the GlcNAc 6-phosphate produced contained one ^{18}O label, indicating that water has added to the sugar moiety (*9*). In addition, an unsaturated sugar was detected upon extended incubation of either MurNAc 6-phosphate or GlcNAc 6-phosphate with MurQ. This species had an absorbance maximum at 235 nm and reacted with both bromine and Ehrlich's reagent. It was assigned to be a 2,3-unsaturated sugar that is generated by the release of the α,β-unsaturated aldehyde intermediate from the active site of the enzyme during catalysis. The notion that MurQ utilizes an enolate-based mechanism is also supported by its assignment as a member of the sugar phosphate isomerase/sugar phosphate binding protein (SIS) family (*7, 9, 11*). Notably, MurQ shares sequence homology with the SIS domain of glucosamine 6-phosphate synthase (GlmS) that serves to generate glucosamine 6-phosphate from fructose 6-phosphate and glutamine (*12*). In the absence of glutamine, GlmS can interconvert glucose 6-phosphate and fructose 6-phosphate via an enolate-based isomerization (*13*).

This work describes further studies of *E. coli* MurQ that support a mechanism involving the *syn* elimination of lactate to give an α,β-unsaturated aldehyde with (*E*)-stereochemistry, followed by the *syn* addition of water to give product. The reaction proceeds with the incorporation of a solvent-derived proton at C2 and a solvent-derived oxygen at C3 (but not at C1). We develop a structural model for *E. coli* MurQ and compare it to the known structure of GlmS to identify the active site of the enzyme. Mutagenesis studies suggest that Glu83 and Glu114 are key acid/base residues, and their respective roles in catalysis are investigated.

EXPERIMENTAL PROCEDURES

Materials and General Methods. Chemicals were purchased from Sigma-Aldrich and used without further purification unless otherwise noted. Flash chromatography was performed using Silica Gel SiliaFlash F60 (230−400 mesh, Silicycle). Pyridine, triethylamine, methylene chloride, and methanol were distilled over CaH_2 under an atmosphere of N_2. ^1H NMR spectra were acquired on a Bruker AV 400 instrument at a field strength of 400 MHz. Mass spectrometry was performed by electrospray ionization (ESI-MS) using an Esquire LC mass spectrometer. Neutral compounds were detected as positive ions, and negatively charged compounds were detected as negative ions. Protein concentrations were determined by the method of Bradford using bovine serum albumin as the standard (*14*).

Overexpression and Purification of Wild-Type E. coli MurQ. Recombinant C-terminal hexahistidine-tagged MurQ was prepared using plasmid pUB9 that has been described

previously (*9*). pUB9 was transformed into chemically competent *E. coli* BL21 cells, which were incubated overnight in 5 mL of Luria-Bertani (LB) medium containing 50 μg/mL ampicillin at 37 °C with shaking at 225 rpm. The overnight cultures were poured into 500 mL of LB medium containing 50 μg/mL ampicillin and incubated at 37 °C with shaking at 225 rpm until an OD_{600} of 0.6−0.8 was reached. Isopropyl β-D-galactopyranoside (IPTG) was added to induce overexpression (0.3 mM), and the cultures were allowed to continue to incubate at 37 °C with shaking at 225 rpm for an additional 4 h. The cells were harvested at 5000 rpm (3800*g*) for 30 min and the pellets snap-frozen in liquid nitrogen and stored at −80 °C. Because of the reported instability of *E. coli* MurQ (*9*), the purified enzyme was not stored for any prolonged period of time but instead prepared freshly before each use according to the following protocol.

For each experiment, a frozen cell pellet was resuspended in 10 mL of lysis buffer [30 mM Na_2HPO_4, 300 mM NaCl, and 3 mM DTT (pH 7.5)] and lysed three times at 20000 psi using an ice-cooled French pressure cell. The cell lysate was centrifuged at 5000 rpm (3800*g*) for 20 min and subsequently passed through a 0.45 and 0.22 μm filter before affinity chromatography. A 10 mL column containing Chelating Sepharose-Fast Flow (GE Healthcare) was charged with 2 column volumes (CV) of 100 mM $NiSO_4$, followed by 2 CV of H_2O, and then 3 CV of running buffer containing 5 mM imidazole [20 mM Na_2HPO_4 and 300 mM NaCl (pH 7.5)]. The filtered cell lysate was loaded onto the column, and 50 mL of running buffer containing 5 mM imidazole was passed through the column, followed by 50 mL of running buffer containing 125 mM imidazole. The hexahistidine-tagged etherase, MurQ, was subsequently eluted with running buffer containing 500 mM imidazole. The enzyme was concentrated by being passed through an Amicon Ultra-4 (Millipore, 10000 MWCO) membrane filter at 5000 rpm (3800*g*). The concentrated enzyme was exchanged into the appropriate buffer by spinning three times through an Amicon Ultra-4 (Millipore, 10000 MWCO) membrane filter at 5000 rpm (3800*g*) with 1 mL of the appropriate buffer. Enzyme purified in this fashion was stored on ice and used for the appropriate experiments within 5 h of purification.

Preparation and Expression of Mutant MurQ Plasmids. Site-directed mutagenesis was carried out essentially as described for the QuikChange kit from Strategene (La Jolla, CA). In brief, to introduce the E83A and D115N point mutations, a pair of complementary oligonucleotides were ordered from MWG Biotech (Ebersber, Germany) that encoded a modified codon at the desired position [E83(GAA) → A83(GCC), D115(GAT) → N115(AAT); for E83A, CTGGGGATTCTGGATGCTAGCGCCTGTC-CGCCCACCTACG (nonmatching nucleotides are underlined; introduction of a silent mutation "T" introduced an additional NheI site); for D115N, GCCATTCAGCACGCG-GTGGAAGGCGCCGAAAATAGCCGGGAAGGCGGTG (nonmatching nucleotides are underlined; introduction of a silent mutation "C" introduced an additional KasI/NarI site)]. The oligonucleotides were used as primers for 18 cycles of in vivo DNA replication of the entire plasmid pUB9 with Pwo polymerase (pQLab, Erlangen, Germany). Subsequently, methylated template DNA was removed with DpnI restriction, and the entire mixture was transformed into competent DH5α cells. To confirm the introduction of the mutation, the plasmid DNA was controlled for cleavage of the restriction site that had been introduced by the mutagenesis primers, and subsequently, the mutagenized region was sequenced. The MurQ mutants E83Q and E114Q were constructed in a similar fashion, but without the incorporation of a restriction site, using the oligonucleotide primers listed below (mutated nucleotides underlined). Oligonucleotide primers for the E83Q mutant were as follows: 5′-CTGGAT-GCCAGCCAGTGTCCGCCCACCTACG-3′ (forward) and 5′-CGTAGGTGGGCGGACACTGGCTGGCATCCAG-3′ (reverse). Primers for the E114Q mutant were as follows: 5′-GGTGGAAGGCGCGCAGGATAGCCGGGAAG-3′ (forward) and 5′-CTTCCCGGCTATCCTGCGCGCCTTCCACC-3′ (reverse). The E83Q and E114Q gene sequences were confirmed through DNA sequencing of the entire gene. Expression of the mutated plasmids and purification of the resulting MurQ mutants were conducted in a fashion identical to that of the wild-type enzyme.

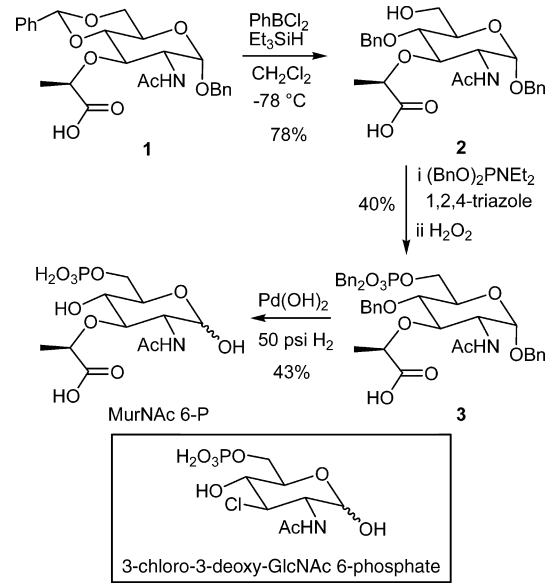

FIGURE 3: Synthesis of MurNAc 6-phosphate. The inset shows the structure of the alternate substrate 3-chloro-3-deoxy-GlcNAc 6-phosphate.

Synthesis of N-Acetylmuramic Acid 6-Phosphate (MurNAc 6-phosphate). MurNAc 6-phosphate was prepared in three steps starting from the literature known compound **1** (Figure 3) (*15*). [2-^{2}H]MurNAc 6-phosphate was prepared in an identical manner starting with the known compound [2-^{2}H]GlcNAc (*16*).

*Benzyl 2-Acetamido-4-O-benzyl-3-O-(D-1-carboxyethyl)-2-deoxy-α-D-glucopyranoside (**2**).* The procedure for the regioselective ring opening of compound **1** was adapted from existing literature methodology (*17*). Compound **1** (666 mg, 1.41 mmol) was dissolved in 50 mL of distilled CH_2Cl_2, and the solution was stirred for 1 h under an argon atmosphere in the presence of 4 Å molecular sieves. The reaction mixture was cooled to −78 °C, and triethylsilane was added (1.35 mL, 8.48 mmol). After 5 min, dichlorophenylborane (1.11 mL, 8.48 mmol) was added to the reaction mixture, and the stirring was continued at −78 °C. The reaction progress was monitored for the disappearance of starting material by TLC analysis (4:1 CH_2Cl_2/MeOH mixture) and was judged to be complete after 2 h. The reaction was quenched at −78 °C with 1.25 mL of NEt_3 and 1.25 mL of MeOH, and the

mixture was allowed to warm to room temperature. The solution was diluted with 25 mL of CH_2Cl_2 and washed twice with 75 mL of cold H_2O and once with 50 mL of saturated NaCl. The aqueous washes were combined and acidified with concentrated HCl and subsequently extracted multiple times with CH_2Cl_2. All organic extracts were pooled and dried over $MgSO_4$ before being concentrated in vacuo. Silica gel chromatography (9:1 CH_2Cl_2/MeOH mixture and then 4:1 CH_2Cl_2/MeOH mixture) gave compound **2** (520 mg, 77%): ^{1}H NMR (400 MHz, MeOD) δ 7.32−7.20 (m, 10H), 5.13 (d, 1H, J = 2.4 Hz), 4.75−4.61 (m, 3H), 4.48−4.39 (m, 2H), 3.80−3.52 (m, 6H), 1.91 (s, 3H), 1.30 (d, 3H, J = 6.8 Hz); ESI-MS m/z 472.3 $[M - H]^-$.

*Benzyl 2-Acetamido-4-O-benzyl-3-O-(*D*-1-carboxyethyl)-2-deoxy-6-O-dibenzylphosphoryl-*α*-*D*-glucopyranoside (***3***).* To a solution of compound **2** (520 mg, 1.10 mmol) in 50 mL of distilled CH_2Cl_2 under an argon atmosphere was added triazole (0.304 g, 4.40 mmol). To this mixture was added dibenzyl *N*,*N*-diethylphosphoramidite (85%, 1.00 g, 2.68 mmol), and the reaction mixture was stirred at room temperature for 3 h. The reaction mixture was diluted with 200 mL of Et_2O and washed with 150 mL each of H_2O and saturated NaCl. The organic layer was dried over $MgSO_4$ and concentrated in vacuo to generate the crude phosphite sugar. The crude phosphite sugar residue was dissolved in 30 mL of THF and cooled to −78 °C before 5 mL of 30% H_2O_2 was added. The reaction mixture was allowed to warm to room temperature, subsequently poured into 120 mL of Et_2O, and successively washed with 3 × 50 mL of ice-cold H_2O and 1 × 60 mL of saturated NaCl. The aqueous washes were pooled and acidified with concentrated HCl and extracted with CH_2Cl_2. The combined organic extracts were dried over $MgSO_4$ and concentrated in vacuo. Silica gel chromatography (CH_2Cl_2, then 9:1 CH_2Cl_2/MeOH mixture, and then 4:1 CH_2Cl_2/MeOH mixture) afforded compound **3** (322 mg, 39.9%): ^{1}H NMR (400 MHz, MeOD) δ 7.37−7.20 (m, 20H), 5.12−5.02 (m, 5H), 4.69−4.53 (m, 3H), 4.50−4.39 (m, 2H), 4.16−4.07 (m, 2H), 3.78−3.68 (m, 3H), 3.46 (dd, 1H, J = 8.8 Hz, J = 9.2 Hz), 1.93 (s, 3H), 1.34 (d, 3H, J = 6.8 Hz); ESI-MS m/z 732.7 $[M - H]^-$.

*2-Acetamido-3-O-(*D*-1-carboxyethyl)-2-deoxy-*α*,*β*-*D*-glucose 6-Dihydrogen Phosphate (MurNAc 6-phosphate).* Compound **3** (410 mg, 0.560 mmol) was hydrogenated (50 psi) over $Pd(OH)_2$ in distilled MeOH with a catalytic amount of acetic acid (60 μL). When the reaction was judged to be complete by MS analysis, the mixture was filtered through a pad of Celite and the filtrate concentrated in vacuo. The residue was dissolved in a minimal amount of MeOH, toluene added, and the mixture concentrated to remove any residual amounts of acetic acid. The residue was dissolved in H_2O and loaded onto a 10 mL column of AG-1X8 resin (formate form). The column was washed with 50 mL each of H_2O and 1.4, 2.8, 4.2, and 5.6 N formic acid, and each of the fractions was analyzed by ESI-MS for the presence of MurNAc 6-phosphate. Fractions found to contain product (collected between 4.2 and 5.6 N formic acid) were pooled, and the volume was reduced on a rotary evaporator. Distilled H_2O was added and the remaining solvent evaporated; this procedure was repeated multiple times to remove any remaining formic acid and gave 90 mg (42%) of MurNAc 6-phosphate. The phosphate sugar was dissolved in 10 mL of H_2O and carefully titrated to pH 7.5 with NaOH. The resulting solution was frozen and lyophilized to give the disodium salt of MurNAc 6-phosphate as a white solid. α-Anomer: ^{1}H NMR (400 MHz, D_2O) δ 5.54 (d, 1H, J = 2.8 Hz), 4.47 (q, 1H, J = 6.8 Hz), 4.04−3.84 (m, 2H), 3.75−3.46 (m, 3H), 2.04 (s, 3H), 1.36 (d, 3H, J = 6.8 Hz). β-Anomer: ^{1}H NMR (400 MHz, D_2O) δ 4.67 (d, 1H, J = 8.4 Hz), 4.30 (q, 1H, J = 6.8 Hz), 4.04−3.84 (m, 2H), 3.75−3.46 (m, 3H), 2.04 (s, 3H), 1.33 (d, 3H, J = 6.8 Hz); ESI-MS m/z 372.3 $[M - H]^-$.

Coupled Kinetic Assay for MurQ Activity. The elimination of D-lactate from *N*-acetylmuramic acid 6-phosphate by MurQ was monitored using a coupled spectrophotometric assay that employs D-lactate dehydrogenase and NAD^+. To ensure the coupling reactions are thermodynamically favorable, the production of NADH was coupled to the reduction of *p*-iodonitrotetrazolium violet (INT) using the enzyme diaphorase (*18*). The rate of D-lactate elimination was followed by monitoring the increase in absorbance at 500 nm (reduced INT) using a Cary 4000 UV−vis spectrophotometer. All kinetic assays were performed at 30 °C in 60 mM Trien-HCl buffer (pH 8) containing 0.65 mM INT, 5 mM NAD^+, 10 units of diaphorase, 30 units of D-lactate dehydrogenase, a variable concentration of *N*-acetylmuramic acid 6-phosphate, and a fixed amount of MurQ (total volume of 1 mL). MurQ dilutions were stabilized by the addition of 5% (v/v) of a 10 mg/mL BSA solution in H_2O and kept on ice before use. Assay mixtures were preincubated at 30 °C for 5 min and then reactions initiated by the addition of a fixed amount of MurQ. A nonlinear lag associated with the coupled assay was observed, and initial velocities were therefore calculated on the basis of the linear slope between 10 and 15 min after initiation using a least-squares analysis with Cary 3 software. Under these conditions, the observed rates changed in direct proportion to the amount of MurQ added and were unaffected by changes in the amount of added coupling enzymes. The extinction coefficient of reduced *p*-iodonitrotetrazolium violet at 500 nm was determined to be 10250 M^{-1} cm^{-1} by adding stock solutions of NADH to the assay mixture and measuring the final absorbance changes. The initial rates were fit to the Michaelis−Menten equation using GraFit, version 4.0, and the kinetic parameters were determined on the basis of this fit.

Monitoring the MurQ Reaction in D_2O Using ^{1}H NMR Spectroscopy. A solution of sodium phosphate buffer prepared with D_2O (25 mM, pD 7.9, 600 μL) and containing MurNAc 6-phosphate (3.75 mM) was placed in an NMR tube, and an initial ^{1}H NMR spectrum was recorded. To this solution was added freshly purified MurQ [40 μg that had been exchanged into 15 μL of the same deuterated buffer using an Ultrafree-0.5 centrifugal filter device (Millipore, 10000 MWCO)], and the reaction mixture was incubated at 37 °C. ^{1}H NMR spectra were acquired at 30 min intervals to monitor the progress of the enzymatic reaction. Spectra taken of control reaction mixtures lacking MurQ showed no change over the course of several days. Incubations with *N*-acetylglucosamine 6-phosphate and 3-chloro-3-deoxy-*N*-acetylglucosamine 6-phosphate were performed in an identical manner; however, additional MurQ was required in the latter case (40 μg in 15 μL of the same buffer).

Reduction of the Unsaturated Intermediate with $NaBH_4$. *N*-Acetylglucosamine 6-phosphate (10 mg) was dissolved in

500 μL of 10 mM phosphate buffer prepared using D_2O (pD 7.9), and wild-type (WT) MurQ (150 μg) was added. The enzymatic mixture was transferred to an NMR tube and incubated at 37 °C for 12 h until equilibrium had been reached. The enzyme was removed by filtration through an Ultrafree-0.5 centrifugal filter device (Millipore, 10000 MWCO) and the filtrate frozen and lyophilized. The residue was dissolved in 1.5 mL of D_2O, $NaBH_4$ (10 mg) added, and the resulting solution heated at 37 °C in a 15 mL Falcon tube. After 3 h, the solution was transferred to an NMR tube and a ^1H NMR spectrum was acquired.

Nonenzymatic Production of an Alkene Intermediate from 3-Chloro-3-Deoxy-GlcNAc 6-Phosphate. A sample of Trien-HCl buffer (200 mM, pH 8) was evaporated to dryness and reconstituted with an equal volume of D_2O. This procedure was repeated four times to ensure that all residual H_2O was removed. A solution of 3-chloro-3-deoxy-GlcNAc 6-phosphate (6 mM, 1.2 mL) was prepared in the resulting buffer and incubated at 42 °C. The reaction was monitored periodically by ^1H NMR spectroscopy for the appearance of characteristic intermediate alkene peaks. After 5 days, the conversion of 3-chloro-3-deoxy-GlcNAc 6-phosphate to alkene intermediate was judged to be complete. The solution of intermediate was used without further purification to test its catalytic competence with both WT MurQ and MurQ mutants.

^{18}O Isotope Incorporation Experiment. *N*-Acetylglucosamine 6-phosphate (17 mg) was dissolved in 500 μL of $H_2{}^{18}O$ (97%, Cambridge Isotope Laboratories) and the solution sealed in a glass tube. The mixture was heated at 60 °C for 5 h, after which analysis by ESI-MS indicated that >95% of the sugar contained 1 equiv of ^{18}O isotope. The solution was snap-frozen in liquid N_2 and lyophilized to dryness. Analysis of the [1-^{18}O]-*N*-acetylglucosamine 6-phosphate by ^1H NMR spectroscopy (D_2O, 400 MHz) gave a spectrum identical to that of unlabeled sample, and it was used for subsequent enzymatic experiments without further purification. A solution of sodium phosphate buffer (20 mM, pH 7.5, 500 μL) containing [1-^{18}O]-*N*-acetylglucosamine 6-phosphate (2.5 mM) was prepared and diluted with $H_2{}^{18}O$ (97%, 500 μL). A sample of MurQ (1.6 mg in 25 μL of the sodium phosphate buffer) was added, and the resulting solution was incubated at 37 °C and monitored for ^{18}O incorporation/washout by ESI-MS.

Structural Modeling of E. coli MurQ and Multiple-Sequence Alignment. The structure of the MurQ homologue *Haemophilus influenzae* HI0754 was elucidated as part of a structural genomics project (P. Kim, P. Quartey, R. Ng, T. I. Zarembinski, and A. Joachimiak, unpublished results; PDB entry 1NRI, posted January 24, 2003). The *E. coli* MurQ structure was modeled using the coordinates of 1NRI (1.90 Å resolution) with SWISS-MODEL 8.05 (*19*). The structural model was refined using MolProbity (*20*) and Coot (*21*); the coordinates as Protein Data Bank files are available on request. MurQ forms stable dimers as seen by gel filtration and dynamic light scattering (T. Jaeger, unpublished results). Accordingly, MurQ was modeled as a homodimer. The putative active site residues of MurQ were identified by comparing the homodimer model with crystal structures of the GlmS isomerase with phosphosugars bound to the active site (entries 1MOQ, 1MOR, and 1MOS) and by multiple-sequence alignment of etherases and the sugar phosphate isomerase/sugar phosphate binding (SIS) domains of GlmS using ClustalW (Figure 8).

Solvent-Derived Deuterium Incorporation into MurNAc 6-Phosphate with WT and E83A MurQ. A solution of *N*-acetylmuramic acid 6-phosphate (6.9 mM) in sodium phosphate buffer prepared with D_2O (25 mM, pD 7.9, 1.60 mL) was divided into two aliquots. To one aliquot was added WT MurQ (5 μg), and to the other was added E83A (40 μg). The samples were transferred to NMR tubes and incubated at 37 °C. The reactions were monitored periodically by NMR spectroscopy to observe any wash-in of deuterium at C2 as evidenced by the collapse of the H1 doublet to a singlet. At each time point, a small aliquot was removed from the reaction mixture and diluted into MeOH for analysis by ESI-MS.

RESULTS

Kinetic Studies and Determination of Isotope Effects. In previous studies on MurQ, kinetic constants could not be obtained due to a lack of access to adequate quantities of the substrate, MurNAc 6-phosphate, which could be obtained only in microgram quantities using MurQ deletion mutants (*9*). To overcome this hurdle, we developed a chemical synthesis of MurNAc 6-phosphate (Figure 3). The known protected version of MurNAc, compound **1**, was prepared in three steps from GlcNAc, as described previously (*15*). A selective ring opening of the benzylidine acetal gave compound **2** with a free hydroxyl at C6 (*17*). This compound was phosphorylated using a phosphoramidite coupling followed by oxidation to give compound **3**. A final deprotection by hydrogenation gave MurNAc 6-phosphate on a 100 mg scale.

The enzyme used in these studies was a recombinant *E. coli* enzyme bearing a C-terminal histidine tag that was overexpressed in *E. coli*. Due to the sensitivity of the purified enzyme toward freezing and prolonged storage, frozen cell pellets were stored at −78 °C and fresh enzyme was purified each day immediately prior to use. Enzyme prepared in this fashion could be stored for several hours at 5 °C without a detectable loss of activity.

To measure the kinetic constants for MurQ, a continuous coupled assay was developed that relied on the detection of released lactate using D-lactate dehydrogenase and NAD^+. To ensure that the oxidation of lactate was irreversible, the production of NADH was coupled to the reduction of *p*-iodonitrotetrazolium violet (INT) using the enzyme diaphorase (*18*). This serves to regenerate the NAD^+ in situ and also to generate the reduced form of INT that absorbs strongly at 500 nm. Using this assay, it was possible to show that the MurQ reaction follows Michaelis−Menten kinetics with the following kinetic parameters: $k_{cat} = 5.7 \pm 0.1\ s^{-1}$, $K_M = 1.20 \pm 0.07$ mM, and $k_{cat}/K_M = 4.8 \times 10^3\ M^{-1}\ s^{-1}$ (Figure 4). The addition of 5 mM EDTA to the assay resulted in only weak inhibition (25% reduction in rate), indicating that metal ions are not required in the MurQ reaction.

With the development of a kinetic assay, it was possible to measure a kinetic isotope effect (KIE) for the reaction of [2-^2H]MurNAc 6-phosphate. To obtain the labeled substrate, [2-^2H]GlcNAc was first prepared using literature procedures (*16*) and then converted into [2-^2H]MurNAc 6-phosphate using the synthesis outlined above (Figure 3). Kinetic

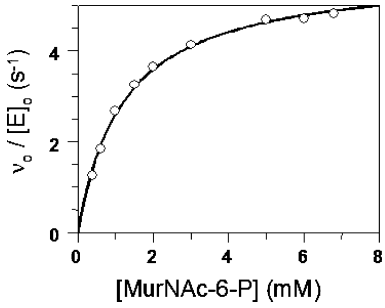

FIGURE 4: Plot of initial velocity vs substrate concentration for the reaction catalyzed by the MurNAc 6-phosphate hydrolase, MurQ. The kinetic parameters obtained by fitting the data to Michealis−Menten kinetics are as follows: $k_{cat} = 5.7 \pm 0.1$ s^{-1}, $K_M = 1.20 \pm 0.07$ mM, and $k_{cat}/K_M = 4.8 \times 10^3$ M^{-1} s^{-1}.

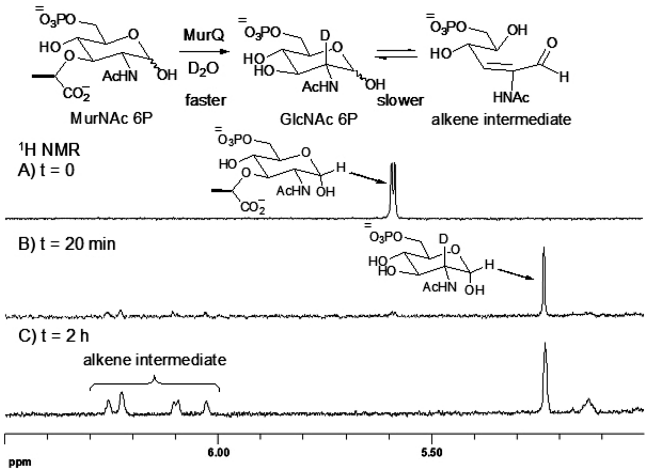

FIGURE 5: ^{1}H NMR spectra from monitoring the reaction of MurNAc 6-phosphate with MurQ in buffered D_2O. (A) Spectrum taken before the addition of enzyme. (B) Spectrum taken after 20 min showing GlcNAc 6-phosphate as the sole product. (C) Spectrum taken after incubation for 2 h showing the appearance of peaks due to the alkene intermediate.

analysis using the coupled assay showed a KIE on the value of k_{cat} to be 1.8 ± 0.1 (k_D/k_H). A KIE of this magnitude can be attributed to a primary KIE on a step that is only partially rate-limiting during catalysis. The observation of a primary KIE with [2-^{2}H]MurNAc 6-phosphate supports a mechanism involving cleavage of the C2−H bond.

Solvent Deuterium Incorporation and Intermediate Release. A key mechanistic study of the MurQ reaction involved conducting the reaction in buffer prepared from D_2O and monitoring its progress using ^{1}H NMR spectroscopy. In this fashion, it was possible to determine whether solvent-derived isotope is incorporated into the C2 position of either starting material or product during the course of the reaction. This experiment was also used to monitor the formation and structure of the unsaturated sugar that was previously reported to be generated during the reaction (*9*). The downfield region of the ^{1}H NMR spectrum taken immediately before the addition of MurQ to a sample of MurNAc 6-phosphate is shown in Figure 5a. The signal due to the anomeric proton of the α-anomer of MurNAc 6-phosphate is seen as a doublet at 5.59 ppm (that of the β-anomer is obscured by the signal of residual HDO). After a 20 min incubation with MurQ, this signal is cleanly converted into a new signal at 5.23 ppm that corresponds to the anomeric proton (α-anomer) of the product GlcNAc 6-phosphate (Figure 5b). No signals other than those attributable to the products GlcNAc 6-phosphate and lactate appeared during this incubation period. The new signal at 5.23 ppm is seen as a singlet indicating that deuterium has been incorporated into the C2 position during catalysis. Mass spectral analysis of the product confirmed that a single nonexchangeable deuterium had been incorporated. This observation supports the elimination mechanism shown in Figure 2 and shows that the proton removed from the C2 position during the elimination of lactate exchanges with solvent during the lifetime of the α,β-unsaturated aldehyde intermediate. In the same experiment, it is possible to monitor the anomeric signal of the MurNAc 6-phosphate as a function of time (not shown in Figure 5). This signal remained a doublet even at the latest stages in the reaction, indicating that deuterium is not incorporated into the C2 position of the starting material at any significant rate. This indicates that once the proton has been removed from C2, the enolate intermediate always proceeds to product (or that the proton cannot exchange with bulk solvent during the lifetime of the enolate).

After further incubation of the reaction mixture, new signals that are attributed to the unsaturated sugar intermediate can be seen to accumulate in the region of the spectrum between 6.3 and 6.0 ppm (Figure 5c). This process eventually reaches a 1:2 unsaturated sugar:GlcNAc 6-phosphate equilibrium ratio, and the identical equilibrium ratio can be obtained when MurQ is incubated with pure GlcNAc 6-phosphate. This intermediate can also be detected by mass spectral analysis and is found to have the same mass as the α,β-unsaturated aldehyde intermediate shown in Figure 2; however, this analysis is complicated by the observation of minor peaks bearing the same mass in spectra of pure GlcNAc 6-phosphate and MurNAc 6-phosphate (presumably as fragmentation products of the molecular ion). These observations indicate that GlcNAc 6-phosphate is the kinetic product of the MurQ reaction and is likely the only relevant one under in vivo conditions. However, upon extended incubation of GlcNAc 6-phosphate with MurQ, the reversible elimination of water occurs, and occasionally, the α,β-unsaturated aldehyde intermediate is released into solution where it accumulates.

Nature of the Unsaturated Sugar Intermediate. The release of the α,β-unsaturated aldehyde intermediate allows one to directly address the stereochemistry of the elimination reactions. If *syn* eliminations were involved, then the intermediate would be an (*E*)-alkene, and if *anti* eliminations were involved, then the intermediate would be a (*Z*)-alkene. It was therefore of interest to examine the structure of the released species in further detail. It is important to note that in the active site of MurQ the α,β-unsaturated aldehyde intermediate must exist in its unhydrated open chain form for the reaction to proceed. However, once it is released into solution, this species could adopt several alternate forms (Figure 6). The open chain form of the (*E*)-α,β-unsaturated aldehyde may be either hydrated or unhydrated, with the latter presumably preferred because of conjugation between the carbonyl and the alkene. This species could also exist in closed chain forms, each of which would give rise to two anomers (the pyranose anomers are boxed in Figure 6). In the case of the (*Z*)-α,β-unsaturated aldehyde, only the open

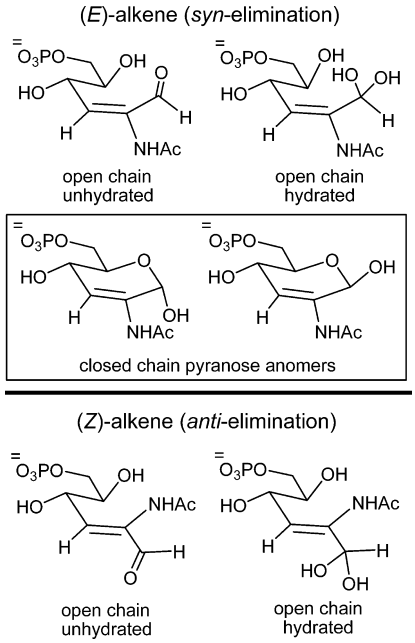

FIGURE 6: Possible structures of the alkene intermediate following its release from the enzyme active site into solution. The top section shows the (*E*)-alkene with the favored structures boxed. The bottom section shows the (*Z*)-alkene.

chain hydrated and unhydrated forms are accessible since ring strain precludes cyclization. The ^{1}H NMR spectrum of a sample containing the unsaturated sugar lacks any aldehydic signals above 7.0 ppm, indicating that the open chain unhydrated forms are not present at any significant level. Long-range COSY and HMQC experiments show that the four signals in the region between 6.3 and 6.0 ppm (Figure 5c) are derived from two species in solution. The downfield signals are due to hemiacetal protons (H1, 6.26 and 6.23 ppm), and the upfield signals are due to alkene protons (H3, 6.10 and 6.03 ppm). Treatment of this mixture with sodium borohydride results in a ^{1}H NMR spectrum containing a single alkene signal (see Figure S1 of the Supporting Information). This indicates that the two unsaturated species share a common alkene geometry. These observations are consistent with the assignment of the unsaturated species as the α- and β-anomers of the closed chain form of the (*E*)-α,β-unsaturated aldehyde (boxed species in Figure 6) and indicate that the MurQ reaction proceeds via *syn* eliminations and additions. While it is possible that the closed chain (*E*)-α,β-unsaturated aldehyde may adopt either the furanose or pyranose form in solution, arguments invoking alkene strain in cyclopentene rings suggest that the pyranose forms would predominate (*22*).

Studies with 3-Chloro-3-Deoxy-GlcNAc 6-Phosphate. To further probe the elimination mechanism proposed for the MurQ reaction, 3-chloro-3-deoxy-*N*-acetylglucosamine 6-phosphate (3-chloro-3-deoxy-GlcNAc 6-phosphate) was investigated as an alternate substrate (Figure 3, inset). It was envisioned that the enzyme would promote the elimination of HCl from this compound and generate the normal (*E*)-α,β-unsaturated aldehyde intermediate that would be readily hydrated to give GlcNAc 6-phosphate. This compound could be very useful in probing the role of the active site acid/base residues since chloride does not require the assistance of an acid catalyst to depart (B_2 in Figure 2).

A benzyl-protected form of the compound was chemically synthesized using a modification of a previously reported procedure (*23, 24*) (see the Supporting Information). Deprotection via hydrogenolysis gave the free compound that was stable to isolation via ion-exchange chromatography. To test for stability of this compound in the absence of enzyme, a sample was incubated in 50 mM phosphate buffer at pH 7.5 and 42 °C and monitored by ^{1}H NMR spectroscopy. The compound was surprisingly stable, and elimination products were observed only after incubation for several hours. The first product to appear displayed an aldehydic signal at 9.28 ppm and an alkene signal at 6.71 ppm (see Figure S2 of the Supporting Information). This was assigned to the unhydrated (*Z*)-α,β-unsaturated aldehyde that results from the *anti* elimination of HCl and must exist in an open chain form (Figure 6). At later time points, signals corresponding to the two pyranose anomers of the (*E*)-α,β-unsaturated aldehyde (Figure 5c) began to appear and eventually dominated the spectrum. This was interpreted as a process in which the (*Z*)-α,β-unsaturated aldehyde was formed as a kinetic product and then gradually isomerized to the (*E*)-α,β-unsaturated aldehyde that is the thermodynamic product. The observation that the (*Z*)-isomer has a significant lifetime in solution indicates that it is not formed as an intermediate in the MurQ reaction or it would have been detected during extended incubations of MurNAc 6-phosphate with the enzyme (Figure 5c). Samples of (*E*)-α,β-unsaturated aldehyde prepared by the nonenzymatic elimination of HCl from 3-chloro-3-deoxy-GlcNAc 6-phosphate were also shown to be catalytically competent and were hydrated by MurQ to give the same 1:2 equilibrium ratio of unsaturated sugar to GlcNAc 6-phosphate seen previously.

When 3-chloro-3-deoxy-GlcNAc 6-phosphate was tested as an alternate substrate for MurQ, a slow conversion into an equilibrium mixture of GlcNAc 6-phosphate and the (*E*)-α,β-unsaturated aldehyde was observed. Control experiments lacking MurQ showed that this process was enzyme-catalyzed and that it occurred with an activity that was approximately 2% of that observed with MurNAc 6-phosphate. Thus, the 3-chloro derivative does act as an alternate substrate for the enzyme; however, the replacement of the 3-lactyl group (or the 3-hydroxy group of the product) with a chlorine dramatically affects the rate of catalysis. This is reminiscent of previous work on enolase where the replacement of phosphoenolpyruvate with 3-chloro-2-phosphoglyceric acid reduced the value of V_{max} by a factor of 600 (*25*).

Solvent-Derived ^{18}O Isotope Incorporation. In past studies, the MurQ reaction was conducted in buffer prepared from $H_2{}^{18}O$ and the resulting GlcNAc 6-phosphate was found to contain 1 equiv of ^{18}O isotope (*9*). While it is reasonable to assume that the label had been incorporated at C3, it was not possible to rule out the notion that it may have been incorporated at C1. Incorporation of solvent isotope at C1 would be expected if the enzyme were to employ a Schiff base mechanism involving formation of an imine linkage between the C1 aldehyde and an active site lysine residue. It should be noted that such a mechanism has been invoked in the GlmS reaction and is therefore a distinct possibility in the case of MurQ (*26*). To distinguish between these two scenarios, a sample of the product GlcNAc 6-phosphate was

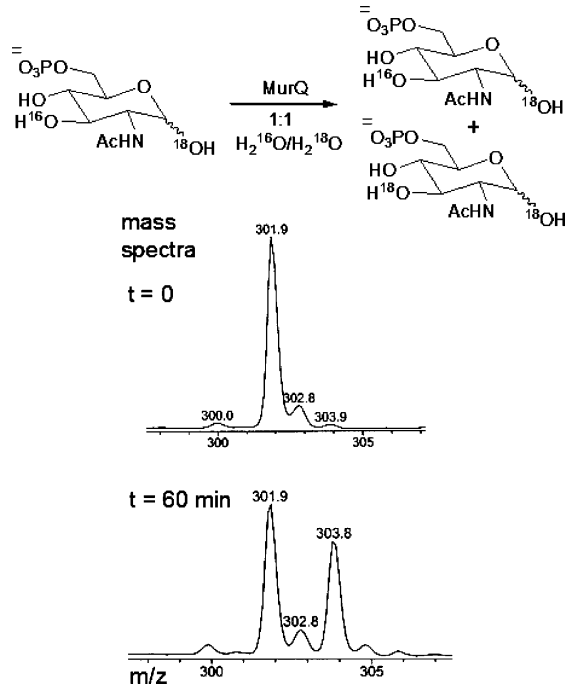

FIGURE 7: Mass spectra showing the reaction of [1-^{18}O]GlcNAc 6-phosphate with MurQ in a buffer prepared from 50% $H_2{}^{16}O$ and 50% $H_2{}^{18}O$: (top) spectrum taken before the addition of enzyme and (bottom) spectrum taken after incubation with MurQ for 60 min.

prepared that contained a >95% incorporation of ^{18}O isotopic label at the C1 position. This was incubated with MurQ in a buffer prepared from 50% $H_2{}^{18}O$ and 50% $H_2{}^{16}O$, and the reaction was monitored by mass spectrometry (Figure 7). The original signal at *m*/*z* 302 was gradually observed to convert into an approximately 50:50 mixture of two signals at *m*/*z* 302 (singly labeled) and *m*/*z* 304 (doubly labeled). The observation of doubly labeled species indicates that the ^{18}O isotope had been washed into the C3 position of GlcNAc 6-phosphate by a reversible dehydration process. The absence of any unlabeled species indicates that there was no washout of the ^{18}O label from the C1 position under these reaction conditions. This finding argues against the formation of a Schiff base intermediate during catalysis.

Structural Comparison of MurQ with GlmS and Identification of Potential Active Site Residues. To identify potential active site residues that could serve as acid/base catalysts during the MurQ reaction (B_1 and B_2 in Figure 2), a structural model for the *E. coli* MurQ was developed. This model was based on the reported structure of a protein of unknown function, *H. influenzae* HI0754, that was determined as part of a structural genomics project (P. Kim, P. Quartey, R. Ng, T. I. Zarembinski, and A. Joachimiak, unpublished results; PDB entry 1NRI). *E. coli* MurQ and *H. influenzae* HI0754 are overall 55% identical in their amino acid sequence and have approximately the same number of residues (298 vs 303). On the basis of the high level of sequence identity with MurQ, it is very likely that HI0754 also functions as a MurNAc-6-phosphate etherase. MurQ forms stable dimers as seen by gel filtration and dynamic light scattering (T. Jaeger, unpublished results). Accordingly, MurQ was modeled as a homodimer (see ref *7*). Both a sequence analysis and the structural model of MurQ indicate that each monomer contains an SIS domain. SIS domains are found in many

Table 1: Kinetic Constants for the Reactions Catalyzed by MurQ and Its Mutants

enzyme	k_{cat} (s^{-1})	K_M (mM)	k_{cat}/K_M (M^{-1} s^{-1})
WT MurQ	5.7 ± 0.1	1.20 ± 0.07	4.8×10^3
Glu83Ala	0.0005 ± 0.0001	—	—
Glu114Gln	0.0028 ± 0.0002	0.32 ± 0.03	8.8
Asp115Asn	0.79 ± 0.01	0.83 ± 0.04	9.5×10^2

sugar−phosphate binding proteins such as isomerases, C−N lyases, and bacterial transcriptional regulators involved in sugar phosphate metabolism (*11*). The overall dimer resembles the structure of glucosamine-6-phosphate synthase (GlmS), a protein that is overall <20% identical to MurQ based on the amino acid sequence. GlmS is a bifunctional enzyme that converts fructose 6-phosphate to glucosamine 6-phosphate, catalyzing the first step in a pathway leading to the eventual formation of amino sugar-containing macromolecules via uridine 5′-diphosphate-*N*-acetylglucosamine (UDP-GlcNAc) (*12*). The N-terminal aminotransferase module of GlmS can be removed, leaving a C-terminal isomerase module, which is functional but catalyzes only an isomerization (fructose 6-phosphate to glucose 6-phosphate). The isomerase domain of GlmS forms a pseudodimer, carrying two SIS domains on one polypeptide strand; the first SIS domain is more closely related to MurQ than the second SIS domain of GlmS (*7*). The isomerase module of GlmS has been extensively studied with regard to mechanism and structure (*12, 13, 27*−*29*). Using the structural model of the *E. coli* homodimer of MurQ and the cocrystal structures of the isomerase module of glucosamine 6-phosphate synthase, along with multiple-sequence alignment (Figure 8), three amino acid residues that were conserved in all putative etherases were identified as candidates for a role in catalysis: Glu83, Glu114, and Asp115. Glu83 is located at the end of helix 1 (H1) that connects β-strands 1 and 2 (S1 and S2) in the $\alpha-\beta-\alpha$ sandwich fold of the SIS domain. It is located at a position similar to Glu488 of GlmS, which was identified as the key acid/base catalyst in that enzyme (*29*). Glu114 and Asp115 of MurQ were located on a short α-helix that carries the His504 of GlmS thought to be involved in sugar ring opening during catalysis (*29*). In GlmS, a lysine residue (Lys603) forms a Schiff base with the aldehyde of the substrate (*26, 29*); however, this residue is not conserved within the etherases (Figure 8).

Characterization of MurQ Mutants. To investigate the role of the putative active site residues, the following MurQ mutants were generated: Glu83Gln, Glu83Ala, Glu114Gln, and Asp115Asn. All four of the MurQ mutants were kinetically characterized using the continuous coupled assay for lactate release (Table 1). The Glu83Gln mutant was devoid of activity; however, the Glu83Ala mutant showed a very low, but measurable, level of activity with a k_{cat} value that was 10000-fold lower than that of the wild-type enzyme (it was not possible to accurately determine the value of K_M for this mutant). The Glu114Gln mutant also showed a dramatic reduction in the value of k_{cat} (2000-fold) and a modest decrease in the value of K_M (4-fold). The Asp115Asn mutant exhibited an only 7-fold reduction in the value of k_{cat} and is therefore not likely serving as a key acid/base residue during catalysis. These findings corroborate the notion that the active site of MurQ is located in the same position as that of GlmS and that the structural model for

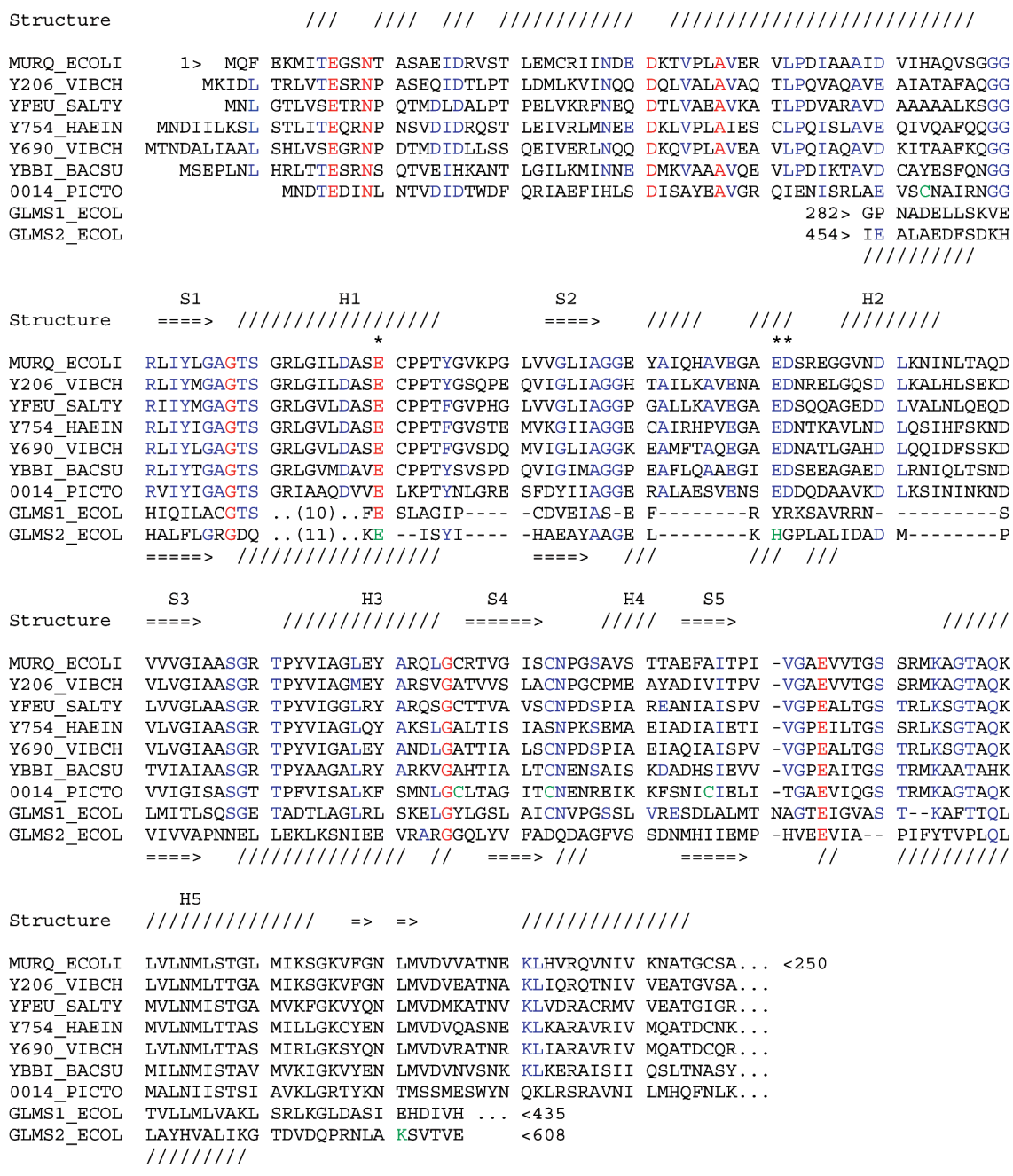

FIGURE 8: Identification of putative active site residues using a multiple-sequence alignment and the structural model of *E. coli* MurQ. The amino acid sequences of the sugar phosphate isomerase/sugar phosphate binding protein (SIS) domains of MurQ of *E. coli* (MURQ_ECOLI) and selected putative MurNAc etherases (*Vibrio cholerae*, Y206_VIBCH and Y690_VICH; *Salmonella thyphi*, YFEU_SALTY; *H. influenzae*, Y754_HAEIN; *Bacillus subtilis*, YBBI_BACSU; *Picrophilus torridus*, 0014_PICTO) are shown along with the two SIS domains of GlmS and the glucosamine-6-phosphate synthase of *E. coli* (GLMS1_ECOLI and GLMS2_ECOLI). Conserved amino acid residues are colored red, and residues that are conserved only within the etherase sequences are colored blue. The active site residues Glu488, His504, and Lys603 of GlmS are colored green. The structural motifs (helices, =>; sheets, ////) of the SIS domain fold (a five-stranded parallel β-sheet flanked by five α-helices) are shown and numbered according to their appearance in the amino acid sequence. Residues E83, E114, and D115 (*E. coli* MurQ numbering) are marked with asterisks.

MurQ is valid. They also implicate Glu83 and Glu114 as reasonable candidates to act as B_1 and B_2 in the MurQ reaction (Figure 2).

To further characterize the reactions catalyzed by Glu83Ala and Glu114Gln, the reactions were carried out in buffered D_2O and continuously monitored by ^1H NMR spectroscopy. With the wild-type enzyme, no incorporation of deuterium into the residual pool of starting material can be detected even after 80% of the reaction has been completed. This indicates that the partitioning of the enolate forward to product occurs more rapidly than exchange of the C2-derived proton with bulk solvent. The results obtained with the Glu83Ala mutant were quite different in that a wash-in of deuterium into the C2 position was found to occur much more rapidly than turnover to product. This is readily apparent in observing that the doublet corresponding to the α-anomeric proton at 5.59 ppm collapses into a singlet before any product signal can be detected at 5.23 ppm (Figure 9). The Glu83Ala-catalyzed incorporation of a single deuterium into MurNAc 6-phosphate was also observed using mass spectrometry. This indicates that the Glu83Ala mutant is

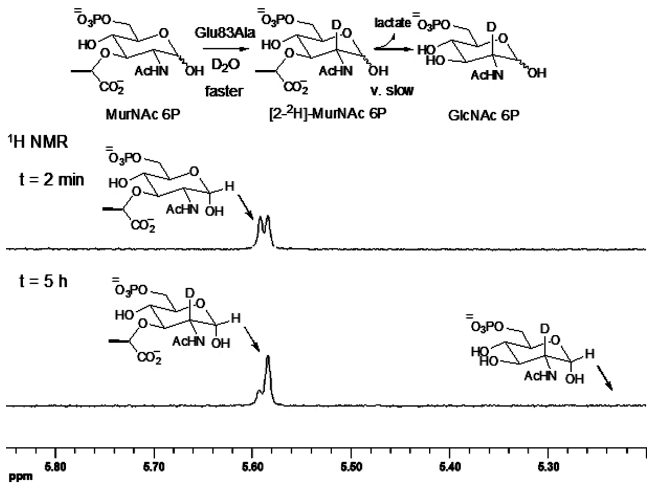

FIGURE 9: ^{1}H NMR spectra from monitoring the reaction of MurNAc 6-phosphate with the Glu83Ala mutant in buffered D_2O: (top) spectrum taken after incubation for 2 min with the mutant showing unlabeled MurNAc 6-phosphate and (bottom) spectrum taken after incubation for 5 h showing the formation of [2-^{2}H]MurNAc 6-phosphate before any GlcNAc 6-phosphate is generated.

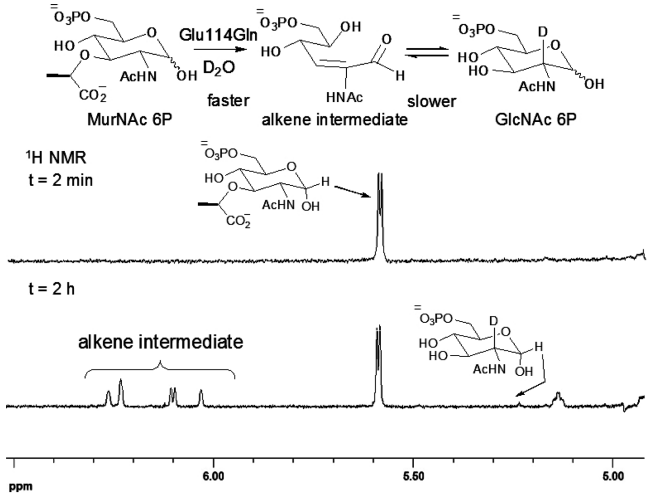

FIGURE 10: ^{1}H NMR spectra from monitoring the reaction of MurNAc 6-phosphate with the Glu114Gln mutant in buffered D_2O: (top) spectrum taken after incubation for 2 min with the mutant showing MurNAc 6-phosphate and (bottom) spectrum taken after incubation for 2 h showing the appearance of the alkene intermediate before significant GlcNAc 6-phosphate is generated.

still capable of removing the proton at C2 to form an enolate intermediate, but since a subsequent step in catalysis is impaired, this proton has time to exchange with bulk solvent before it is returned to give labeled starting material. This scenario presents Glu83 as a reasonable candidate to serve as B_2 in Figure 2.

The results obtained with the Glu114Gln mutant also differed significantly from those of the wild-type enzyme. In the latter case, the first formed product was GlcNAc 6-phosphate and the α,β-unsaturated aldehyde intermediate accumulated only after extended incubation (Figure 5). However, with the Glu114Gln mutant, the first formed product is the α,β-unsaturated aldehyde intermediate. This is clearly shown in Figure 10, where the signals due to the unsaturated intermediate at 6.3−6.0 ppm appear before those of the product GlcNAc 6-phosphate at 5.23 ppm (α-anomeric proton). The fact that intermediate release is faster than catalysis with this mutant is likely due to a crucial role for Glu114 in catalyzing the hydration of the intermediate (as either B_1 or B_2 in Figure 2). Once the intermediate is formed (albeit slowly) by the irreversible elimination of lactate, it is more likely to be released from the active site than proceed to product when subsequent steps of catalysis are impaired by the mutation.

The Glu83Ala and Glu114 Gln mutants were also tested for their ability to accept 3-chloro-3-deoxy-GlcNAc 6-phosphate as an alternate substrate. We anticipated that a mutant lacking B_2 (Figure 2) would still be able to promote the elimination of HCl from this compound at a rate comparable to that of the wild-type enzyme since acid catalysis would not be required. However, even with extended incubations, no enzyme-catalyzed elimination could be detected with either of these mutants.

DISCUSSION

The studies outlined here are in full agreement with the proposed MurQ mechanism (Figure 2). The existence of a primary KIE in the reaction of [2-^{2}H]MurNAc 6-phosphate, and the observed incorporation of solvent-derived deuterium into the product GlcNAc 6-phosphate, both indicate that cleavage of the C2−H bond accompanies catalysis. The incorporation of the solvent-derived ^{18}O isotope into the C3 position, but not the C1 position, indicates that cleavage of the C3−O bond also occurs and that formation of a Schiff base is not involved. Together these studies support an elimination−addition mechanism involving an α,β-unsaturated aldehyde intermediate. This mechanism is also supported by the findings that 3-chloro-3-deoxy-GlcNAc 6-phosphate serves as an alternate substrate (via an elimination of HCl) and that a 2,3-alkene accumulates upon extended incubation of GlcNAc 6-phosphate with the enzyme. The observation that synthetic samples of the 2,3-alkene are hydrated by MurQ to give GlcNAc 6-phosphate demonstrates that this is a catalytically competent species and, therefore, the true reaction intermediate. Spectroscopic analysis of the intermediate is consistent with an alkene bearing an (*E*)-configuration, indicating that the reaction proceeds via a *syn* elimination of lactate followed by a *syn* addition of water. This agrees with past studies showing that eliminations involving more acidic protons adjacent to thioesters, ketones, and aldehydes generally occur via *syn* stereochemistry, whereas those operating adjacent to carboxylates employ *anti* stereochemistry (*30, 31*). While ample mechanistic precedence exists for each of the half-reactions catalyzed by MurQ, the overall hydrolysis of an ether via an E1cb-like elimination−hydration process is quite rare in enzymology (*10*). The first half of the MurQ reaction is similar to the reactions catalyzed by C−O lyases such as carboxymethyloxysuccinate lyase (*32*) and the polysaccharide lyases that operate on uronic acids (*33*). The second half of the MurQ reaction is similar to that of the β-hydratases such as enoyl-CoA hydratase that catalyzes the *syn* hydration of an α,β-unsaturated thioester (*34*−*36*). Perhaps the closest precedence for the MurQ mechanism is found in the family 4 glycosidases that employ a transient oxidation strategy and elimination−hydration chemistry to cleave glycosidic bonds (*33, 37*).

The finding that MurQ can be assigned to the sugar phosphate isomerase/sugar phosphate binding protein (SIS)

family is also consistent with the proposed mechanism (*7, 9, 11*). The sugar phosphate isomerases generally operate via carbanionic intermediates and involve deprotonations adjacent to carbonyl or iminium functional groups. The observation that MurQ shares a significant degree of sequence identity with the *H. influenzae* HI0754 protein of known structure enabled the development of a structural model of MurQ. This structure was further modeled as a homodimer to resemble the pseudodimeric structure of GlmS, and this proved to be useful in identifying active site residues. In this fashion, Glu83 and Glu114 were identified as key catalytic residues in the MurQ reaction. A direct comparison between the roles of individual residues in the GlmS reaction to those in the MurQ reaction is somewhat tenuous given the low level of sequence identity between the two enzymes and the differences in the chemical reactions catalyzed. GlmS binds glucosamine 6-phosphate and isomerizes it to give the imine derivative of fructose 6-phosphate (*12, 29*). It can also isomerize glucose 6-phosphate to give fructose 6-phosphate (*13*). In each case, a deprotonation at C2 initiates catalysis and a protonation at C1 completes catalysis. The key active site residue involved in both of these proton transfers is provided by Glu488 which is the structural homologue to Glu83 in the model of MurQ. With this argument, the role of Glu83 in the MurQ reaction would be to deprotonate the C2 position of MurNAc 6-phosphate (B_1 in Figure 2). The solvent deuterium incorporation results with the Glu83Ala mutant, however, paint a somewhat different picture. The observation that the Glu83Ala mutant is essentially devoid of hydrolase activity yet capable of exchanging the C2 proton of substrate with solvent-derived protons suggests that it plays a role other than that of C2 deprotonation. A likely possibility is that it assists in lactate departure (B_2 in Figure 2). The role of Glu114 is not completely clear from these studies; however, it seems evident that this residue plays a key role in both the elimination and hydration steps of the reaction (possibly as B_1) since the release of lactate was slowed considerably and the intermediate was released into solution before hydration could take place. Further studies on the role of active site residues, including identification of candidates that assist ring opening of the sugar, will be greatly aided by a cocrystal structure of MurQ with bound substrate or intermediate analogues.

SUPPORTING INFORMATION AVAILABLE

Description of the synthesis of 3-chloro-3-deoxy-GlcNAc 6-phosphate, ^{1}H NMR spectra showing the reduction of the alkene intermediate and the nonenzymatic decomposition of 3-chloro-3-deoxy-GlcNAc 6-phosphate, and ^{1}H NMR spectra of synthetic products. This material is available free of charge via the Internet at http://pubs.acs.org.

REFERENCES

1. Vollmer, W., Blanot, D., and de Pedro, M. A. (2008) Peptidoglycan structure and architecture. *FEBS Microbiol. Rev. 32*, 149–167.
2. Park, J. T. (1996) The Murein Sacculus. In *Escherichia coli and Salmonella: Cellular and Molecular Biology* (Neidhardt, F. C., Curtis, R., III, Ingraham, J. L., Lin, E. C. C., Low, K. B., Magasanik, B., Resnikoff, W. S., Riley, M., Schaechter, M., and Umbarger, H. E., Eds.) pp 48−57, American Society for Microbiology, Washington, DC.
3. Höltje, J.-V. (1998) Growth of the stress-bearing and shape-maintaining murein sacculus of *Escherichia coli*. *Microbiol. Mol. Biol. Rev. 62*, 181–203.
4. Park, J. T., and Uehara, T. (2008) How bacteria consume their own exoskeletons (turnover and recycling of cell wall peptidoglycan). *Microbiol. Mol. Biol. Rev. 72*, 211–227.
5. Shockman, G. D., Daneo-Moore, L., Kariyama, R., and Massidda, O. (1996) Bacterial walls, peptidoglycan hydrolases, autolysins, and autolysis. *Microb. Drug Resist. 2*, 95–98.
6. Uehara, T., Suefuji, K., Valbuena, N., Meehan, B., Donegan, M., and Park, J. T. (2005) Recycling of the anhydro-*N*-acetylmuramic acid derived from cell wall murein involves a two-step conversion to N-acetylglucosamine-phosphate. *J. Bacteriol. 187*, 3643–3649.
7. Jaeger, T., and Mayer, C. (2008) N-Acetylmuramic acid 6-phosphate lyases (MurNAc etherases): Role in cell wall metabolism, distribution, structure, and mechanism. *Cell. Mol. Life Sci. 65*, 928–939.
8. Uehara, T., Suefuji, K., Jaeger, T., Mayer, C., and Park, J. T. (2006) MurQ etherase is required by *Escherichia coli* in order to metabolize anhydro-N-acetylmuramic acid obtained either from the envrionment or from its own cell wall. *J. Bacteriol. 188*, 1660–1662.
9. Jaeger, T., Arsic, M., and Mayer, C. (2005) Scission of the lactyl ether bond of N-acetylmuramic acid by *Escherichia coli* "etherase". *J. Biol. Chem. 280*, 30100–30106.
10. White, G. F., Russell, N. J., and Tidswell, E. C. (1996) Bacterial scission of ether bonds. *Microbiol. Rev. 60*, 216–232.
11. Bateman, A. (1999) The SIS domain: A phosphosugar-binding domain. *Trends Biochem. Sci. 24*, 94–95.
12. Durand, P., Golinelli-Pimpaneau, B., Mouilleron, S., Badet, B., and Badet-Denisot, M.-A. (2008) Highlights of glucosamine-6P synthase catalysis. *Arch. Biochem. Biophys. 474*, 302–307.
13. Leriche, C., Badet-Denisot, M.-A., and Badet, B. (1996) Characterization of a phosphoglucose isomerase-like activity associated with the carboxy-terminal domain of *Escherichia coli* glucosamine-6-phosphate synthase. *J. Am. Chem. Soc. 118*, 1797–1798.
14. Bradford, M. M. (1976) A rapid and sensitive method for the quantitation of microgram quantities of protein utilizing the principle of protein-dye binding. *Anal. Biochem. 72*, 248–254.
15. Flowers, H. M., and Jeanloz, R. W. (1963) The synthesis of 2-acetamido-3-*O*-(D-1-carboxyethyl)-2-deoxy-α-D-glucose (*N*-acetylmuramic acid) and of benzyl glycoside derivatives of 2-amino-3-*O*-(D-1-carboethyl)-2-deoxy-α-D-glucose (muramic acid). *J. Org. Chem. 28*, 2983–2986.
16. Hanchak, M., and Korytnyk, W. (1976) Studies on the epimerization of 2-acetamido-2-deoxy-D-glucopyranose: Selective deuteration of C-2 of 2-acetamido-2-deoxyaldoses. *Carbohydr. Res. 52*, 219–222.
17. Sakagami, M., and Hamana, H. (2000) A selective ring opening reaction of 4,6-*O*-benzylidene acetals in carbohydrates using trialkylsilane derivatives. *Tetrahedron Lett. 41*, 5547–5551.
18. Rej, R. (1982) A convenient continuous-rate spectroscopic method for determination of amino-acid substrate-specificity of aminotransferases: Application to isoenzymes of aspartate-aminotransferase. *Anal. Biochem. 119*, 205–210.
19. Arnold, K., Bordoli, L., Kopp, J., and Schwede, T. (2006) The SWISS-MODEL workspace: A web-based environment for protein structure homology modeling. *Bioinformatics 22*, 195–201.
20. Lovell, S. C., Davis, I. W., Arendall, W. B., III, deBakker, P. I. W., Word, J. M., Prisant, M. G., Richardson, J. S., and Richardson, D. C. (2003) Structure validation by C-α geometry: ϕ, ψ, and C-β deviation. *Proteins: Struct., Funct., Genet. 50*, 437–450.
21. Emsley, P., and Cowtan, K. (2004) Coot: Model-building tools for molecular graphics. *Acta Crystallogr. D60*, 2126–2132.
22. Wiberg, K. B. (1986) The concept of strain in organic chemistry. *Angew. Chem., Int. Ed. 25*, 312–322.
23. Spohr, U., and Zu Reckendorf, W. M. (1982) Di- and polyamino sugars. XXX. Reaction of a 2,3-anhydro sugar with a 6-amino sugar, synthesis and reactions of a *N*-[glycos-6-yl]epimino sugar. *Liebigs Ann. Chem. 7*, 1375–1383.
24. Ali, Y., Richardson, A. C., Gibbs, C. F., and Hough, L. (1968) Some further ring-opening reactions of methyl 4,6-O-benzylidene-2,3-dideoxy-2,3-epimino-α-D-allopyranoside and its derivatives. *Carbohydr. Res. 7*, 255–271.

25. Stubbe, J., and Abeles, R. H. (1980) Mechanism of action of enolase: Effect of the β-hydroxy group on the rate of dissociation of the α-carbon-hydrogen bond. *Biochemistry 19*, 5505–5512.
26. Golinelli-Pimpaneau, B., and Badet, B. (1991) Possible involvement of Lys603 from *Escherichia coli* glucosamine-6-phosphate synthase in the binding of its substrate fructose 6-phosphate. *Eur. J. Biochem. 201*, 175–182.
27. Wojciechowski, M., Milewski, S., Mazerski, J., and Borowski, E. (2005) Glucosamine-6-phosphate synthase, a novel target for antifungal agents. Molecular modelling studies in drug design. *Acta Biochim. Pol. 52*, 647–653.
28. Bearne, S. L., and Blouin, C. (2000) Inhibition of *Escherichia coli* glucosamine-6-phosphate synthase by reactive intermediate analogs. *J. Biol. Chem. 275*, 135–140.
29. Teplyakov, A., Obmolova, G., Badet-Denisot, M.-A., and Badet, B. (1999) The mechanism of sugar phosphate isomerization by glucosamine 6-phosphate synthase. *Protein Sci. 8*, 596–602.
30. Mohrig, J. R., Moerke, K. A., Cloutier, D. L., Lane, B. D., Person, E. C., and Onasch, T. B. (1995) Importance of historical contingency in the stereochemistry of hydratase-dehydratase enzymes. *Science 269*, 527–529.
31. Widlanski, T., Bender, S. L., and Knowles, J. R. (1989) Dehydroquinate synthase: The use of substrate analogues to probe the late steps of the catalyzed reaction. *Biochemistry 28*, 7572–7582.
32. Peterson, D., and Llaneza, J. (1974) Identification of a carbon-oxygen lyase activity cleaving ether linkage in carboxymethoxysuccinic acid. *Arch. Biochem. Biophys. 162*, 135–146.
33. Yip, V. L., and Withers, S. G. (2006) Breakdown of oligosaccharides by the process of elimination. *Curr. Opin. Chem. Biol. 10*, 147–155.
34. Agnihotri, G., and Liu, H.-W. (2003) Enoyl-CoA hydratase: Reaction, mechanism, and inhibition. *Bioorg. Med. Chem. 11*, 9–20.
35. Holden, H. M., Benning, M. M., Haller, T., and Gerlt, J. A. (2001) The crotonase superfamily: Divergently related enzymes that catlyze different reactions involving acyl coenzyme A thioesters. *Acc. Chem. Res. 34*, 145–147.
36. Hofstein, H. A., Feng, Y. G., Anderson, V. E., and Tonge, P. J. (1999) Role of glutamate 144 and glutamate 164 in the catalytic mechanism of enoyl-CoA hydratase. *Biochemistry 38*, 9508–9516.
37. Yip, V. L. Y., Varrot, A., Davies, G. J., Rajan, S. S., Yang, X. J., Thompson, J., Anderson, W. F., and Withers, S. G. (2004) An unusual mechanism of glycoside hydrolysis involving redox and elimination steps by a family 4 β-glycosidase from *Thermatoga maritima*. *J. Am. Chem. Soc. 126*, 8354–8355.

BI8014532